Controlled and Regioselective Ring-Opening Polymerization for Poly(disulfide)s by Anion-Binding Catalysis

Tianyi Du,‡ Boming Shen,‡ Jieyu Dai, Miaomiao Zhang, Xingjian Chen, Peiyuan Yu*, Yun Liu*

Abstract:

Poly(disulfide)s are an emerging class of sulfur-containing polymers with applications in medicine, energy, and functional materials. However, the constituent dynamic covalent S−S bond is highly reactive in the presence of sulfide (RS^-) anion, imposing a persistent challenge to control the polymerization. Here, we report an anion-binding approach to arrest the high reactivity of RS^- chain end to control the synthesis of linear poly(disulfide)s, realizing a rapid, living ring-opening polymerization of 1,2-dithiolanes with narrow dispersity and high regioregularity ($M_w/M_n \sim 1.1$, $P_s \sim 0.85$). Mechanistic studies support the formation of a thiourea-base-sulfide ternary complex as the catalytically active species during the chain propagation. Theoretical analyses reveal a synergistic catalytic model where the catalyst preorganizes the protonated base and anionic chain end to establish spatial confinement over the bound monomer, effecting the observed regioselectivity. The catalytic system is amenable to monomers with various functional groups, and semicrystalline polymers are also obtained from lipoic acid derivatives by enhancing the regioregularity.

INTRODUCTION

Sulfur-containing polymers exhibit a myriad of unique properties and functions, leveraging on the desirable physical properties of the S atom and rich reactivity profile of the element. Sulfur-containing polymers come in many shapes and forms, including thioesters,[1-3] thiocarbonates,[4] thioethers,[5] thioamides,[6] thioureas,[7] disulfides,[8] trisulfides,[9] and polysulfides.[10,11] In particular, disulfides (RS−SR) show a gamut of stimuli-responsive properties with only two atoms. Its dynamic covalent nature is robust and media-tolerant,[12,13] making it a popularly sought-after motif in designing functional polymers and already so in nature's macromolecules. For instance, poly(disulfide)s from lipoic acid derivatives have been widely used in biomedical research owing to their biocompatibility and ease of modification. Examples include intracellular delivery of bioactive cargos,[14-20] development of protein conjugates,[21] prodrugs,[22,23] and antibacterials.[24] The past decades also witnessed the surge of applications for disulfide-containing polymers in dynamic materials[25] including supramolecular assemblies,[26-29] liquid crystals,[30] hydrogels,[31-34] supersoft elastomers,[35] pressure-sensitive adhesives,[36] recyclable polymers,[37,38] elastic ceramics,[39] plastic compatibilization,[40] and Li−S batteries.[41] Regardless of its broad utility, synthesis of poly(disulfide)s with controlled weight distribution and backbone regiochemistry remains persistently challenging.

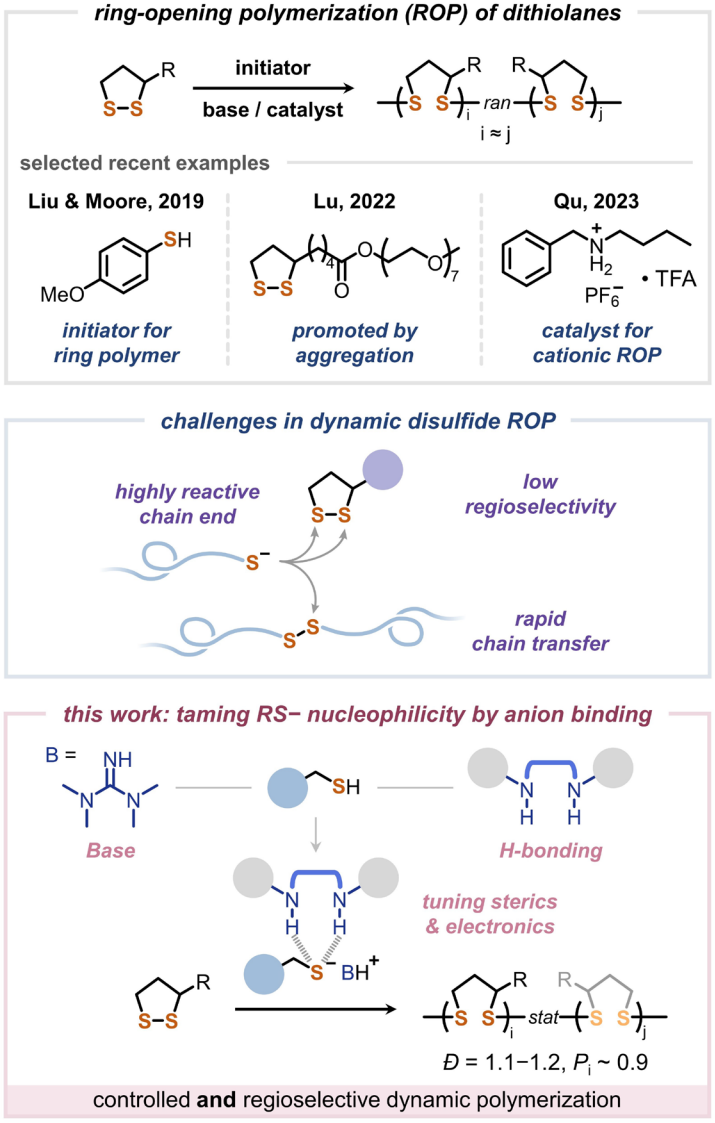

Figure 1. Controlled and regioselective ROP of 1,2-dithiolanes via anion-binding catalysis.

The conventional methods for poly(disulfide)s synthesis include oxidative polycondensation of dithiols,[42,43] thermally induced polymerization in bulk,[44,45] and disulfide exchange.[46,47] Some approaches circumvent the direct construction of S−S bonds by polymerization of monomer with pre-installed disulfide bonds[48,49] or copolymerization with sulfur.[50] Recently, the anionic ring-opening polymerization (ROP) of 1,2-dithiolanes has emerged

as a promising method to synthesize poly(disulfide)s in a more controlled manner.[37,51] Liu and Moore found that using a thiolate initiator (RS^-) with high nucleofugality in the anionic ROP lead to poly(disulfide)s with a cyclic toplogy.[37] Lu showed monomer aggregation as a means to effect grafting-from polymerization at a low monomer concentration from exposed thiolates on the protein surfaces.[17,21] Qu discovered an alternative, cationic ROP of 1,2-diothiolanes, yielding poly(disulfide)s with high molecular weights.[52] Despite recent progress in anionic ROP, the fundamental challenges in controlling the polymerization remain unsolved (Figure 1, central box): the highly nucleophilic sulfide chain end reacts readily with S–S bonds on either monomer or polymer with low selectivity, leading to significant chain transfer and regiochemically irregular polymer backbone.[37,43] The lack of synthetic approach to control the mass distribution and regiochemistry raises a significant barrier to develop functional poly(disulfide) materials with defined structure and composition.

Anion-binding catalysis is a powerful tool that regulates the reactivity of anionic intermediates in small-molecule organic synthesis[53-63] to achieve high chemical selectivity. NH hydrogen bond donors, such as urea and thiourea, prevail in the design of anion-binding catalysts,[64-67] though other hydrogen-bond donors such as OH[68] and CH[69,70] have also been demonstrated. Waymouth and Hedrick pioneered the use of (thio)urea catalysts in the ROP of lactones or lactides to activate monomers and minimize chain transfer.[71-74] Chen carried out kinetic resolution polymerization using a bifunctional chiral thiourea.[75] In these early works, the hydrogen-bond donors were used to directly activate neutral electrophilic substrates via LUMO-lowering effect. The anion-binding approach complements the conventional use of H-bond donors by interacting with the negatively charged nucleophilic species in the polymerization. Wang and Tao used thioureas to stabilize the carboxylate chain end to access controlled anionic ROP of *O*-

carboxyanhydrides[76] and *N*-carboxyanhydrides.[77] Fors extended the use of anion-binding catalyst, thiophosphoramide, to arrest the reactive countercation and furbish an air-tolerant cationic polymerization of vinyl ethers.[78] Recently, Tao applied selenocyclodiphosphazanes as an anion receptor to abstract Cl^- to reversibly activate and deactivate the chain end for living cationic polymerization of vinyl ethers.[79,80] These prior examples of NH-based catalysts exploited a variety of means to control polymerization, inspiring us to strategize anion-binding catalysis in the ROP of 1,2-dithiolanes.

Scheme 1. Regioisomeric Triads in Poly(disulfide)s from 3-Substituted Monomers[a]

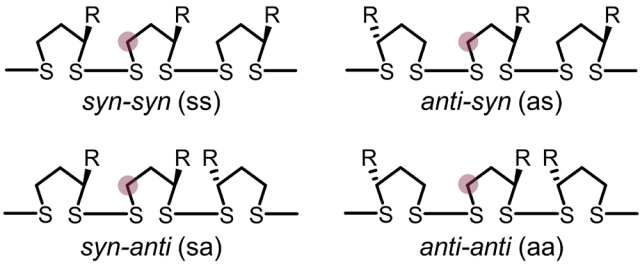

[a]Purple circles highlight ^{13}C signals that are used to calculate triad population (*P*).

Herein, we propose that forming an anion-binding complex with the reactive sulfide[81,82] chain end will modulate its nucleophilicity. The hydrogen-bonding interactions are envisioned to mitigate the negative charge on the RS^- chain end to better its selectivity towards ring-opening (chain propagation) over chain transfer. The complex also casts a sterically crowded environment around the monomer upon binding, improving the regioselectivity of the ring-opening reaction. To identify polymerization conditions that are ideal for the formation of anion-binding complex, we selected (*R*)-methyl lipoate, **(*R*)-LM**, as the model ring-opening monomer for its structural simplicity and ease of synthesis from commercially available (*R*)-lipoic acid. The enantiopure monomer also eliminates stereochemical uncertainty from our studies of regioselectivity. The

regioregularity for poly[(***R*)-LM**)] was experimentally measured by the population (P_{ss}) of the regioregular triad, the *syn-syn* triad, by peak deconvolution analysis on ^{13}C NMR data (Scheme 1).[37] This value is then used to calculate the regioselectivity of the ring-opening reaction (P_s).

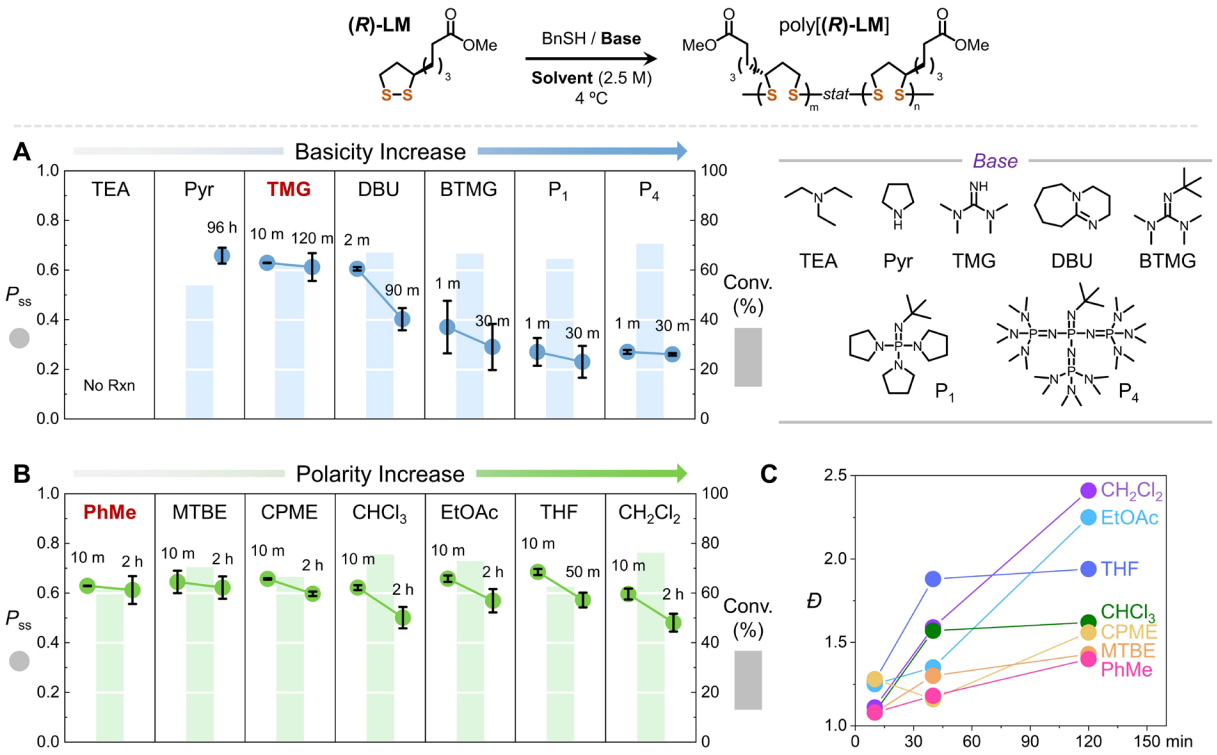

Figure 2. Optimization of ion-pairing interactions for ROP of **(*R*)-LM**. (A) Screening of bases with toluene (PhMe) as solvent. (B) Screening of solvents with tetramethylguanidine (TMG) as base. (C) Dispersity of polymers versus reaction time in different solvents. The circles represent regioregularity (P_{ss}) and the columns represent monomer conversion at the second time point for each entry. Condition: $[Monomer]_0:[Base]_0:[BnSH]_0 = 400:1:1$, $[Monomer]_0 = 2.5$ M, 4 ºC.

RESULTS AND DISCUSSION

Initial Optimization of Base and Solvent. Since it has been established that thiolate (RS^-), not free thiol (RSH), triggers the disulfide exchange for the ring-opening step in the ROP

of 1,2-dithiolanes,[12,17,31,37,83,84] the polymerization of **(*R*)-LM** was tested first with seven commercially available organic bases of varied basicity in nonpolar toluene (Figure 2A). A weak base such as triethylamine (TEA) failed to initiate polymerization while stronger bases succeeded and were observed to reach equilibrium conversion in a shorter time.[85] We also observed that the regioregularity (P_{ss}) decreased and faltered more readily approaching equilibrium for stronger bases.[86] Amongst the seven bases, tetramethyl guanidine (TMG) stroke the best balance between reactivity and control. Then, the polymerization of **(*R*)-LM** was tested with seven common organic solvents of varied polarity, using TMG as base (Figure 2B). The monomer conversion was insensitive to polarity, and the regioregularity slumped by a greater extent in a more polar solvent, though its onset values were similar in different solvents. We hypothesized that the decrease in regioregularity on reaction time is related to chain transfer. Consistently, the dispersity ($Đ$) of poly[**(*R*)-LM**] was found to increase over time in all solvents, and more so in solvent with a higher polarity (Figure 2C). This observation suggests chain transfer reaction has a lower regioselectivity than propagation, and its inhibition is key to better P_{ss}. Overall, TMG was identified as the working base and toluene was selected as the working solvent.

Living Polymerization with Improved Regioselectivity by H-Bonding Catalysts (HBCs). Under the optimized solvent–base combination (TMG/PhMe), we next screened aryl HBCs of different NH donors such as urea, thiourea, squaramide, and sulfonamide (Figure S20). Polymerization was slowed down with these HBCs or even inhibited when using squaramide and sulfonamide, suggesting that binding of RS^- chain end lowers its reactivity. The initial screening showed that the unsymmetric bis-thiourea (Scheme 2), **TU$_{2ch}$**, provides good control over polymerization to reach a dispersity ($Đ$) as low as 1.08,[87] but at the cost of reactivity as evident by the lower conversion (38% *vs.* typical 60–70%). Using **TU$_{2ch}$**, we found that the

dependence of regioregularity or dispersity on base remained similar with and without HBC, and so does the solvent polarity (Figure S22), although the magnitude of impact was mitigated in the presence of HBC. This phenomenon implies that the base and the HBC are playing different and complementary roles in polymerization control.

Scheme 2. The Chemical Structures of Representative H-Bonding Catalysts and Monomers

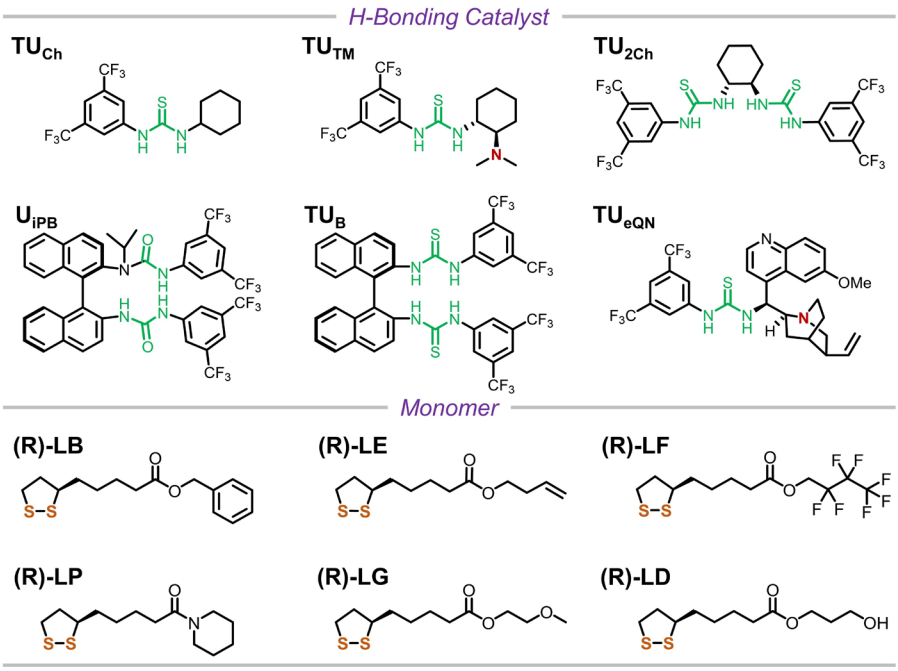

We then turned to HBC with a stereochemically defined binding pocket with an envision that such catalyst effects better regioselectivity of ROP (Table 1). Initial test using multiple NH donors with a chiral skeleton was counterproductive (Figure 3A): the BINAM-based thiourea catalyst with four NH donors, **TU$_B$**, was shown to inhibit polymerization (Table 1, entry 3), while the monosubstituted urea catalyst with three NH donors, **U$_{iPB}$** (Table 1, entry 5), showed expedited conversion (40%) compared to **TU$_{2ch}$** (20%) at 40 min (Table 1, entry 4). The improved reactivity still jeopardizes regioselectivity. For instance, catalyst with further decreasing number of NH donors, such as **TU$_{ch}$** with two donors, showed a faster conversion (50% at 40 min) and a greater

drop in regioregularity ($\Delta P_{ss} = -0.1$) than **TU$_{2ch}$**, which showed 20% conversion with no decrease in P_{ss} under the same condition (Figure S19). Serendipitously, we found that unsymmetric thioureas with tertiary amines as extra hydrogen bond acceptor resolves the reactivity-selectivity dilemma. Takemoto's catalyst (**TU$_{TM}$**) maintained a high regioselectivity until ~60% conversion (Table 1, entry 6 and Figure S33). Finally, thiourea with epiquinine motif, **TU$_{eQN}$**, achieved an excellent regioselectivity ($P_{ss} = 0.7$) and a high reactivity (70% conversion at 40 min; Table 1, entry 7). The **TU$_{eQN}$**-catalyzed ROP of **(*R*)-LM** is 3-fold as fast as **TU$_{2ch}$**, $k = 3.2$ *vs*. 1.1 h^{-1} (Figure 3B), fitted using a previously established propagation kinetic model of a reversible polymerization.[32] The controlled polymerization process was demonstrated by the linear relationship between the molecular weight of poly[**(*R*)-LM**] and monomer conversion along with a persistently low dispersity, $Đ \sim 1.1$ (Figure 3C). A linear increase was also observed for the molecular weight of poly[**(*R*)-LM**] under increasing monomer-to-initiator ratio (Figure 3D), indicating a good chain end fidelity. Indeed, the end groups was confirmed by matrix-assisted laser desorption/ionization-time-of-flight (MALDI-TOF) mass spectrometry to be the initiator and the quencher (Figure S36).

With a controlled polymerization at hand, we now have access to how the polymerization loses control due to chain transfer. Noted that undesirable introduction of other disulfide, likely from the oxidation of initiator thiol, can be an additional source of chain transfer; therefore, the purity of thiol is critical for controlled polymerization. The low regioselectivity of chain transfer (*vide supra*) yields polymer chains with two propagating chain ends, which was observed by MALDI-TOF and gel permeation chromatography (GPC) as a high-molecular-weight shoulder to the main peak (see Supporting Information S.10). Upon extending the reaction time well past 70% conversion to reach equilibrium conversion of ~80%, this shoulder peak grew to merge with the

main one, leading to an overall broadened product peak with a poor dispersity (Figure S40). This observation suggests that our control over dispersity benefits from significant suppression of chain transfer and proper timing to stop the reaction before chain transfer regains.

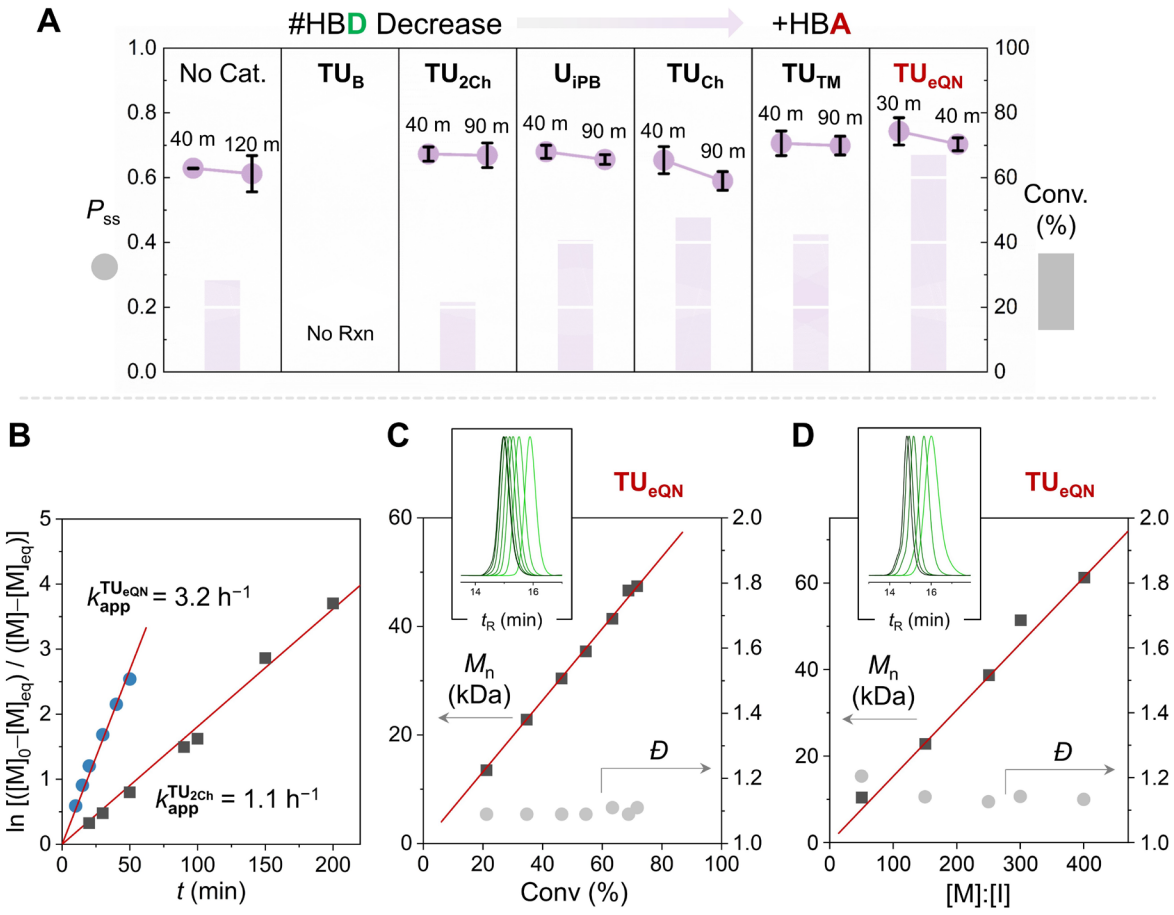

Figure 3. Controlled and regioselective ROP of **(*R*)-LM** via the use of HBCs. (A) Screening of HBCs with varied number of hydrogen bond donors and acceptors. The circles represent regioregularity (P_{ss}), and the columns represent monomer conversion at the first time point for each HBC. Condition: $[Monomer]_0$:$[TMG]_0$:$[BnSH]_0$:$[HBC]_0$ = 400:1:1:5, $[Monomer]_0$ = 2.5 M, PhMe, 4 ºC. (B) Kinetics of ROP using **TU$_{2Ch}$** and **TU$_{eQN}$** as catalyst, and their apparent pseudo-first-order rate constants (k_{app}) determined by ^{1}H NMR. M_n (squares) and $Đ$ (circles) versus (C) monomer conversion or (D) monomer-to-initiator ratio for poly[**(*R*)-LM**)] from **TU$_{eQN}$**-catalyzed ROP. Insets: Corresponding GPC traces of crude polymers (green to black).

Table 1. Summary of HBC-catalyzed ROP of (R)-lipoic acid derivatives[a]

Entry	Monomer	HBC	T (°C)	Time (min)	Conv. (%)[b]	$M_{n,theo}$ (kDa)[c]	$M_{n,exp}$ (kDa)[d]	$Đ$[d]	P_{ss}[e]	P_s[f]
1	**LM**	-[g]	4	120	61	54.3	60.7	1.40	0.61	0.74
2	**LM**	**TU$_{Ch}$**	4	90	69	61.1	44.5	1.16	0.59	0.74
3	**LM**	**TU$_{B}$**	4	90	< 1	-	-	-	-	-
4	**LM**	**TU$_{2Ch}$**	4	90	38	33.7	42.8	1.08	0.67	0.78
5	**LM**	**U$_{iPB}$**	4	90	58	51.8	42.3	1.23	0.66	0.78
6	**LM**	**TU$_{TM}$**	4	90	63	56.1	48.5	1.14	0.70	0.81
7	**LM**	**TU$_{eQN}$**	4	40	72	63.9	50.7	1.15	0.72	0.84
8[h]	**LM**	**TU$_{eQN}$**	4	40	< 1	-	-	-	-	-
9[i]	**LM**	**TU$_{eQN}$**	4	40	< 1	-	-	-	-	-
10	**LM**	**TU$_{eQN}$**	–10	60	75	66.5	86.2	1.08	0.78	0.86
11	**LM**	**TU$_{eQN}$**	–35	90	86	75.5	123.3	1.10	0.84	0.89
12	**LM**	**TU$_{eQN}$**	–45	120	53	47.3	82.5	1.18	0.87	0.92
13	**LB**	**TU$_{eQN}$**	4	40	57	67.8	83.2	1.11	0.76	0.85
14	**LE**	**TU$_{eQN}$**	4	40	64	66.9	82.0	1.15	0.73	0.84
15	**LF**	**TU$_{eQN}$**	4	30	71	110.3	93.5	1.16	0.75	0.84
16	**LP**	**TU$_{eQN}$**	4	240	40	44.4	39.5	1.12	0.64	0.78
17	**LG**	**TU$_{eQN}$**	4	40	63	66.5	66.8	1.11	0.73	0.84
18	**LD**	**TU$_{eQN}$**	4	30	35[j]	37.1	88.2	1.14	0.60	0.75

[a]Polymerization condition: [(***R***)-**LM**]$_0$: [TMG]$_0$: [BnSH]$_0$: [HBC]$_0$ = 400:1:1:5, [(***R***)-**LM**]$_0$ = 2.5 M, PhMe, quenched with *m*-ClPhNCO. [b]Monomer conversion was determined by ^{1}H NMR spectroscopy. [c]Theoritical Molecular weight ($M_{n\ theo}$) was calculated as $M_{n,theo}$ = MW(Monomer) × 400 × Conv. + MW(BnSH) + MW(*m*-ClPhNCO). [d]Determined by GPC analysis using polystyrene standards. [e]Quantified by the ^{13}C NMR data using peak deconvolution as described in section S.3. [f]Ring-opening regioselectivity, calculation detailed in section S.12. [g]Without HBC. [h]Without TMG, [(***R***)-**LM**]$_0$: [BnSH]$_0$: [**TU$_{eQN}$**]$_0$ = 100:1:1. [i]Without TMG and BnSH, [(***R***)-**LM**]$_0$: [**TU$_{eQN}$**]$_0$ = 100:1. [j]Isolated yield.

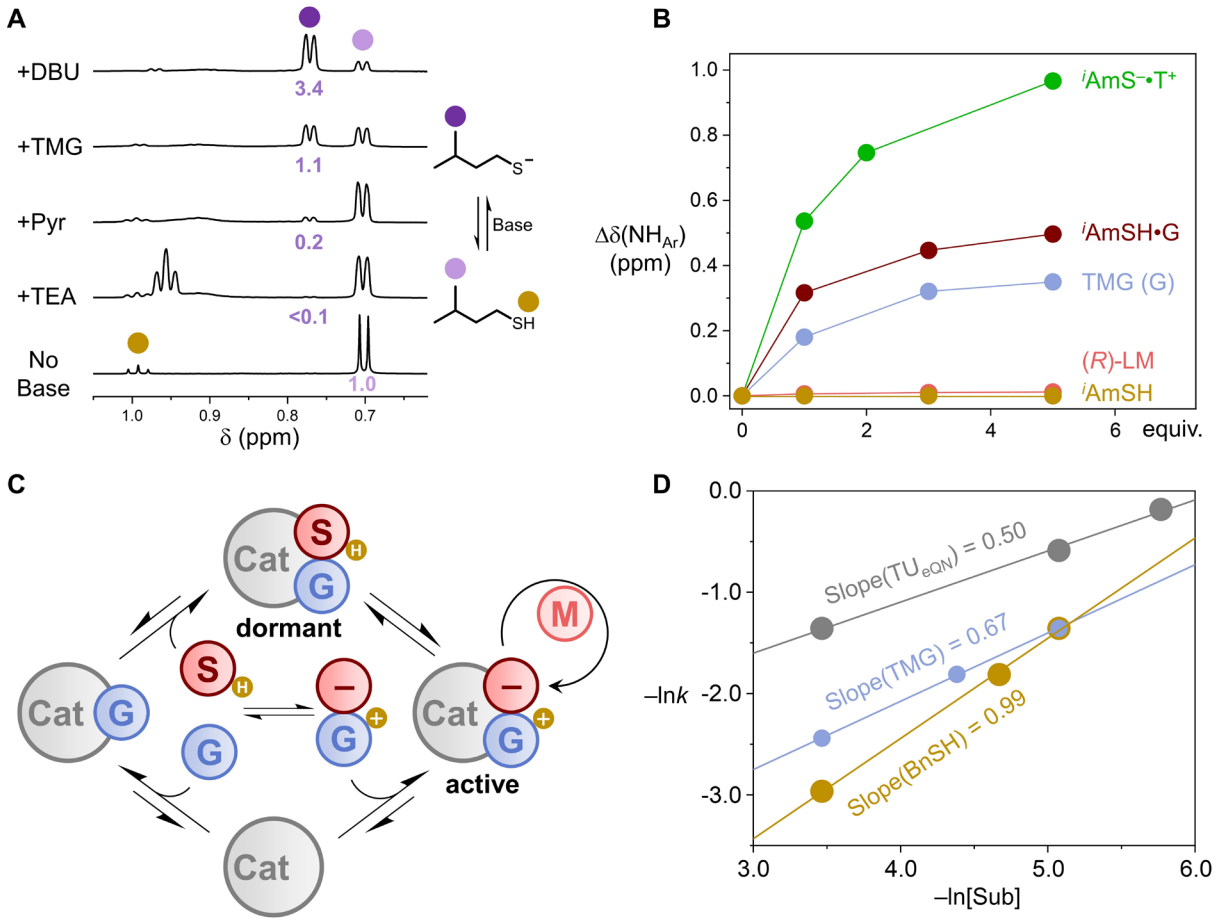

Figure 4. Propagating species in **TU$_{eQN}$**/TMG-mediated anionic ROP. (A) ^{1}H NMR spectra of different thiol-base mixtures (20 mM, PhMe-d_8, 298 K, 600 MHz). (B) Changes in chemical shifts of NH_{Ar} as a function of guest equivalent (5 mM, PhMe-d_8, 298 K, 600 MHz). T^+: tetraethylammonium, NEt_4^+. (C) Proposed chemical equilibrium leading to the formation of propagating species for the controlled ROP (Cat: **TU$_{eQN}$**, G: TMG, S: thiol chain end, M: monomer). (D) Double logarithm plots between apparent propagation rate and concentration of key substance, whose corresponding reaction orders are indicated by the slope.

Experimental Investigation of the Propagating Species. In order to reveal how HBC participates in the anion-binding catalysis, we first evaluated the formation of sulfide anions

in the presence of base (Figure 4A). With increasing basicity, the degree of deprotonation also increased in *i*-amyl thiol, a model thiol selected instead of benzyl thiol for its distinctive NMR resonance peaks after deprotonation. Although the deprotonation of thiol was incomplete by TMG (~50%), the SH proton peak was nearly absent in the NMR spectrum suggesting rapid proton exchange. It has been known that proton can serve as a reversible chain transfer or termination agent in anionic ROP,[88,89] we therefore attributed the ability of TMG to achieve the best control over polymerization amongst screened bases (*cf*. Figure 2) to its appropriate degree of deprotonation and rate of proton exchange. In most cases, we observed slightly higher experimental molecular weights indicative of good initiation efficiencies (>80%) for the **TU$_{eQN}$**/TMG system, suggesting the proton exchange is indeed faster than the propagation and that the reversible termination or chain transfer is contributing to the controlled polymerization. Furthermore, the degree of deprotonation correlates positively to the rate of ROP triggered by these bases (*cf*. Figure 2), consistent with the anionic nature of the propagating species. Finally, the role of TMG as the only base in the catalytic system was confirmed by no-TMG control experiments, where we observed no polymerization (Table 1, entries 8−9; Figure S42) excluding **TU$_{eQN}$**'s role as base.

We then investigated the host-guest interactions between **TU$_{eQN}$** and all other components in the polymerization reaction. To do so, we synthesized a model thiolate, tetraethyl ammonium iso-amyl sulfide, to serve as a fully deprotonated thiolate reference compounds, and performed ^{1}H NMR titrations of this salt with **TU$_{eQN}$** (Figure 4B). We observed clear NH•••S^{-} hydrogen bonding interactions between the thiourea and the thiolate anion, indicated by the downfield shift of NH proton peaks.[79,81] The downfield shift and the sharpening of NH peaks upon thiolate addition indicates that the thiourea was not deprotonated by the sulfide anion, which would have led to

disappearance of the NH peaks.[72] The 1:1 mixture of thiol and TMG induced about half of the magnitude of chemical shift changes in comparison to the thiolate salt, consistent with its degree of deprotonation (Figure 4A). TMG also formed complexes with thiourea, indicated by significant shifts of NH peaks; while nearly no changes in NH peaks suggest minimal hydrogen-bonding interactions with neutral thiol or the **(*R*)-LM** monomer. These observations allowed us to picture the binding equilibrium leading to the propagating species (Figure 4C): **TU$_{eQN}$** (Cat) binds either the thiol-base ion pair (G•SH) or just the base (G). The HBC-bound TMG (Cat•G) can in principle uptake a thiol to form a dormant species (Cat•G•SH). The proton in the ternary complex, Cat•G•SH, is rapidly and reversibly exchanged in an intramolecular or intermolecular fashion to establish an equilibrium between the dormant and the activated form of the catalytic complex, Cat•(GH^+S^-), which then sustains a living and controlled propagation.

The rate law of chain propagation was determined by kinetic measurements under the condition of excess monomer while changing the equivalent of BnSH, TMG, and **TU$_{eQN}$**, respectively (equation 1; Figure 4D; Figure S43):

$$-\mathrm{d}[\textbf{(}\textit{R}\textbf{)-LM}]/\mathrm{dt} = k_p[\mathrm{BnSH}]^{0.99}[\mathrm{TMG}]^{0.67}[\textbf{TU}_{\textbf{eQN}}]^{0.5} \quad (1)$$

The fractional reaction order is often a result of off-cycle ground-state associations,[90-93] which is possible in the current system given the sophisticated association equilibrium depicted in Figure 4C. Nonetheless, the observation of positive reaction orders that do not exceed *unity* for all three species is consistent with their unimolecular participance, i.e., a 1:1:1 stoichiometry, in the rate-determining transition state during propagation, supporting the formation of the proposed catalytic complex as the effective propagating species.

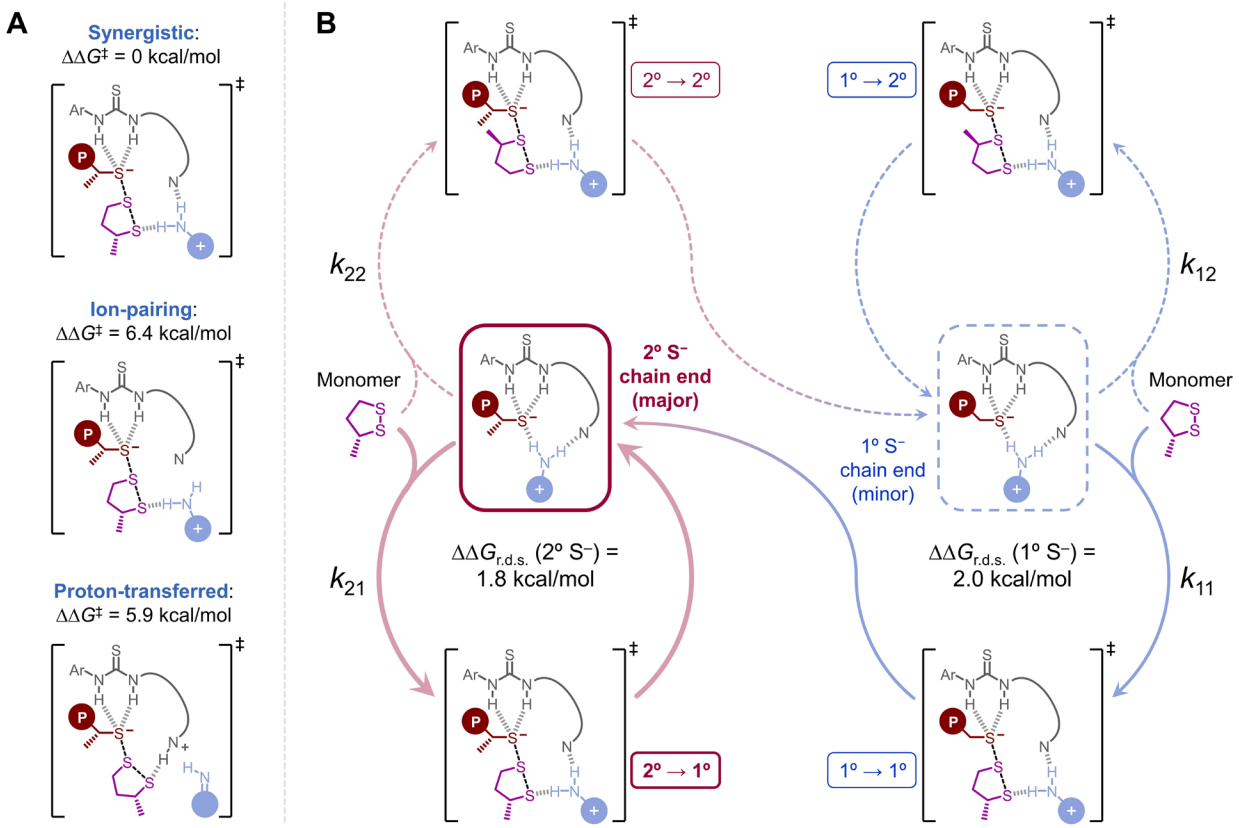

Figure 5. Computational analysis on **TU$_{eQN}$**-catalyzed chain propagation. (A) Relative free energies of TSs associated with different propagation mechanisms. (B) Four possible regiochemical outcomes for chain propagation. Key interactions involved in the resting states and the TSs are shown, along with the corresponding rate-determining span differences ($\Delta\Delta G_{r.d.s.}$) for each chain end computed at the M06-2X/6-311+G(d,p)//ωB97XD/6-31G(d) level of theory using SMD (toluene) solvation model. The monomer is modeled as (*R*)-3-methyl-1,2-dithiolane; the 2° RS$^-$ is modeled as ^{i}PrS$^-$, and the 1° RS$^-$ is modeled as MeS$^-$.

Theoretical and Computational Studies of Regioselectivity in Chain Propagation. Having identified the ternary complex as the propagation species, we shifted our focus to understand how the complex mediates a regioselective chain propagation. We initially proposed three chemically relevant transition states (TSs) for the ring-opening propagation

reaction: a synergistic TS where all species are hydrogen-bonded, an ion-pairing TS where the cation is not associated with **TU**$_{eQN}$, and a proton-transferred TS where the HBC's amine is protonated to serve as the countercation (Figure 5A). The DFT calculations showed that the synergistic TS is the most stable amongst three and was assigned the working TS for ring-opening propagation, while the ion-pairing and proton-transferred TSs are ~6 kcal/mol higher in energy (Figure 5A and Figure S49). Then the rate-determining spans between resting states of **TU**$_{eQN}$-bound RS$^-$ chain end and the working TSs were computed for all four regiochemical combinations (Figure 5B): two types of reactive S in the monomer and two types of RS$^-$ chain end lead to four possible chain growth pathways. The barrier heights for ring-opening reactions are in the range of 9−12 kcal/mol (Figures S45−S46), indicative of an easily accessible process. In contrast, the barrier of chain transfer is significantly higher ($\Delta G^{\ddagger}$ =17.6 kcal/mol, Figure S52), showing that chain transfer is kinetically unfavorable in comparison with chain growth under anion-binding catalysis.

In order to evaluate the computed reaction mechanism based on the synergistic TS, a kinetic model that relates experimental outcomes to elementary propagation reactions are needed. Inspired by the statistical model established in stereoselective polymerization,[94,95] a rate-based statistical model for regioselective polymerization was formulated here. All four ring-opening regiochemistry is considered (Figure 5B). The two pathways from the same type of chain end (1º or 2º RS$^-$) are directly competing, and the outcome of this competition is determined by the ratio of the rate constants. On the basis of steady-state and equal-activity hypotheses, the RS$^-$ chain ends are treated to have stable concentrations during chain growth and their reactivity are independent from the sequence. Then, the probability of regioisomeric triad is expressed as a function of rate constants of elementary propagation reactions (see Supporting Information S.12 for detail

derivation). The assignment of the three regiochemically irregular triads could not be determined directly from experiment.[96] By randomly assigning them on ^{13}C NMR spectra, only one specific assignment consistently yielded, in all tested data sets, non-negative ring-opening rate constants (Table S1) with a ranking order that agrees with literature report.[84,97] The regioisomeric triad successfully assigned, the regioselectivity of the ring-opening reaction, P_s, were obtained by solving the statistical model using the experimentally obtained triad populations (Table 1; Table S2). The experimentally-backed propagation rate constants offer a reference to assess the accuracy of DFT calculations on model ring-opening reactions. The relative rate-determining span ($\Delta\Delta G^{\ddagger}$) for the competing growth pathways from the dominant 2º RS^- chain end (90% population) was computed to be 1.8 kcal/mol. This is in a good agreement with the theoretically derived rate constant ratio (k_{21} / k_{22} = 9) from **TU$_{eQN}$**-catalyzed ROP, which has a regioregularity of 0.7.

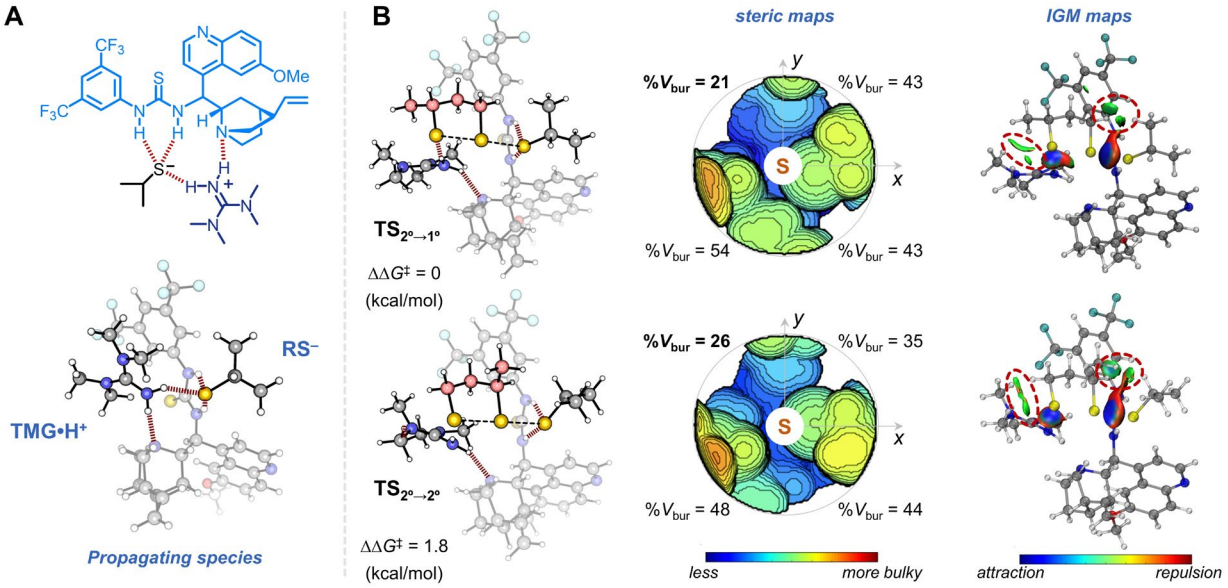

Figure 6. Structural analysis of the ring-opening regioselectivity. (A) The optimized geometry of the HBC-bound RS^- chain end. (B) The transition-state structures of the ring-opening reactions from the 2º RS^- chain ends. The steric maps for the binding pocket of **TU$_{eQN}$** at the TS were

computed using the central S atom in thiolate-disulfide exchange reaction as the center (radius = 5 Å). The intermolecular interactions are shown by independent gradient model (IGM).

Structural analysis was carried out to understand the origin of regioselectivity in **TU$_{eQN}$**-catalyzed ROP. At the resting state, the HBC binds the guanidinium sulfide to form a hydrogen-bonded complex, in which the thiourea's NH donors bind RS$^-$ chain end on the east while the tertiary amine of **TU$_{eQN}$** stabilizes the guanidinium cation on the west (Figure 6A). At the TS, the guanidinium and sulfide chain end dissociates to open up a binding pocket in the north-west quadrant for monomer binding and chain growth (Figure 6B). The available space in the north-west quadrant is evident by its lowest buried volume in the steric maps: %V_{bur} = 21% and 26%, respectively for the two ring-opening pathways from the dominant 2º RS$^-$ chain end. Noncovalent interactions between the monomer and the catalytic complex were revealed by the independent gradient model (IGM) analysis. Two steric contacts were found: one between the cation and the monomer on the west, and the other between monomer and the catalyst on the east. These contacts are greater for the 2º→2º ring-opening regiochemistry than the 2º→1º, as the substituent on the monomer is protruding against the interior of the binding pocket, forcing itself to be in an axial position relative to the ring. The steric crowding by the catalytic pocket and the unfavorable monomer conformation in the 2º→2º TS contribute to the regioselectivity in **TU$_{eQN}$**-catalyzed ROP in favor of 2º→1º ring-opening.

Expanding the Scope and Utility of Controlled Dynamic Polymerization. To examine the versatility of **TU$_{eQN}$**-catalyzed ROP, a range of lipoic acid derivatives were tested as ring-opening monomers (Scheme 2). The monomer scope covers carboxylates with aromatic, alkenyl, fluorous, glycol, and hydroxyl pendent groups and secondary amide. All monomers were successfully polymerized with excellent control ($Đ$ = 1.11−1.16) and high regioregularity (P_{ss} =

0.60−0.76) (Table 1, entries 13–18). Further improvement on regioregularity is possible by lowering the reaction temperature; tighter anion binding and greater ring-opening selectivity are both in favor of higher P_{ss}. Accordingly, the P_{ss} was boosted from 0.7 to 0.86 as the temperature was lowered from 4 to −35 ºC (Figure 7A; Table 1, entries 10–12) but further lowering of the temperature to at −45 ºC increased viscosity and subsided reactivity.

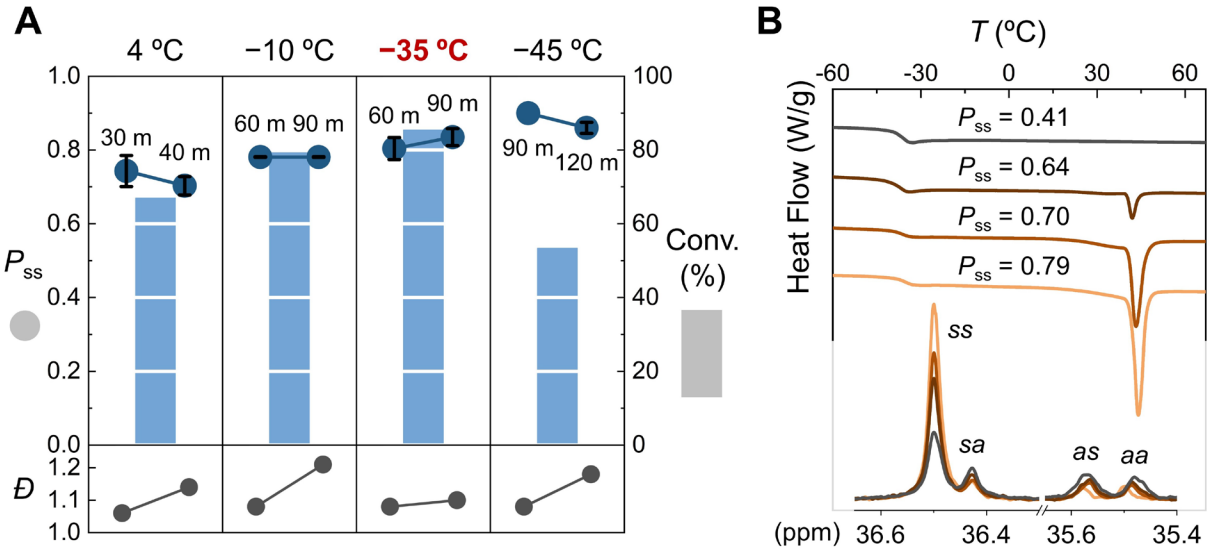

Figure 7. Scope and utility of living regioselective ROP of 1,2-dithiolanes. (A) Impact of temperature on **TU$_{eQN}$**-catalyzed ROP of **(*R*)-LM**. The circles represent regioregularity (P_{ss}), and the columns represent monomer conversion at the second time point for each temperature. (B) DSC traces for poly[**(*R*)-LM**] of varied P_{ss}, and the corresponding ^{13}C NMR spectra showing the region most indicative of regioisomeric triads (Scheme 1).

The improvement of regioregularity is anticipated to benefit thermal properties of poly(disulfide)s. The widely used lipoate monomers were long thought to form amorphous polymers and have been used as a soft segment in copolymerization with the crystalline 1,2-dithiane.[46] The glass transition temperature of poly[**(*R*)-LM**] was shown by differential scanning

calorimetry (DSC) to be around –35 ºC and was not affected by the regioregularity (Figure 7B). Interestingly, with sufficiently high regioregularity (P_{ss} > 0.6, Figure 7B), poly[**(*R*)-LM**] exhibited crystallinity with a melting temperature around 45 ºC, in stark contrast with the anticipation based on its long, flexible side chains. The dependence of crystallinity on regioregularity is an underappreciated idea, and control over polymer's regioregularity now offers a complementary means to tune crystallinity.

CONCLUSION

In conclusion, a controlled and regioselective polymerization of cyclic disulfides have been successfully achieved using a robust TMG/**TU$_{eQN}$** catalytic system. The complex formed between the thiourea catalyst, guanidine base, and thiolate chain end is key. The control over the anionic ROP, demonstrated by the narrow dispersity, is attributed to both the reversible termination by protonated TMG and the NH•••S$^-$ hydrogen bonding interactions offered by catalyst **TU$_{eQN}$**, leading to an improved selectivity for ring-opening reaction over the thiolate-disulfide exchange with the linear S−S bonds in the polymer backbone. The preorganized binding pocket, though assembled by noncovalent interactions and may be perceived as flexible, still led to facilitated distinction of S sites on the lipoate monomers to afford polymers with high regioregularity and improved thermal properties. The catalytic system is shown to be amenable with monomers of varied functional groups, opening doors to control the synthesis of poly(disulfide)s for advanced structures, materials, and applications.

ASSOCIATED CONTENT

Supporting Information

Experimental and computational procedures, synthesis and characterization of new compounds, GPC and NMR data for polymerization of different conditions, experimental studies on polymerization mechanism, theoretical analysis of regioregularity, computational results, and XYZ coordinates (PDF)

AUTHOR INFORMATION

Corresponding Author

Peiyuan Yu − *Department of Chemistry and Shenzhen Grubbs Institute, Southern University of Science and Technology, Shenzhen, 518000, China*; ORCID: 0000-0002-4367-6866; Email: yupy@sustech.edu.cn

Yun Liu − *Beijing National Laboratory for Molecular Sciences, Center for Soft Matter Science and Engineering, Key Laboratory of Polymer Chemistry and Physics of Ministry of Education, College of Chemistry and Molecular Engineering, Peking University, Beijing 100871, China*; ORCID: 0000-0001-7077-363X; Email: yun.liu@pku.edu.cn

Authors

Tianyi Du − *Beijing National Laboratory for Molecular Sciences, Center for Soft Matter Science and Engineering, Key Laboratory of Polymer Chemistry and Physics of Ministry of Education, College of Chemistry and Molecular Engineering, Peking University, Beijing 100871, China*

Boming Shen− *Department of Chemistry and Shenzhen Grubbs Institute, Southern University of Science and Technology, Shenzhen, 518000, China*

Jieyu Dai − *Beijing National Laboratory for Molecular Sciences, Center for Soft Matter Science and Engineering, Key Laboratory of Polymer Chemistry and Physics of Ministry*

of Education, College of Chemistry and Molecular Engineering, Peking University, Beijing 100871, China

Miaomiao Zhang − *Beijing National Laboratory for Molecular Sciences, Center for Soft Matter Science and Engineering, Key Laboratory of Polymer Chemistry and Physics of Ministry of Education, College of Chemistry and Molecular Engineering, Peking University, Beijing 100871, China*

Xingjian Chen − *Beijing National Laboratory for Molecular Sciences, Center for Soft Matter Science and Engineering, Key Laboratory of Polymer Chemistry and Physics of Ministry of Education, College of Chemistry and Molecular Engineering, Peking University, Beijing 100871, China*

Author Contributions

‡These authors contributed equally.

Notes

The authors declare no competing financial interest.

ACKNOWLEDGMENTS

This work was supported by the National Natural Science Foundation of China (22271005), the startup funds from College of Chemistry and Molecular Engineering at Peking University and Beijing National Laboratory for Molecular Sciences. B.S. and Y.P. acknowledge the financial support from Guangdong Basic and Applied Basic Research Foundation (2021A1515010387). Y.L. thanks Prof. Yan Xu and Prof. Rong Zhu for the helpful discussion. We thank Prof. Rong Zhu for access to their GPC instrument. We thank the Beijing NMR Center at Peking University and Dr. Jingxin Yang and Dr. Hongwei Li for the assistance with ^{13}C NMR experiments. Computational work was supported by Center for Computational Science and Engineering, and

the CHEM high-performance supercomputer cluster (CHEM-HPC) of Department of Chemistry, Southern University of Science and Technology.

REFERENCES

(1) Xiong, W.; Chang, W.; Shi, D.; Yang, L.; Tian, Z.; Wang, H.; Zhang, Z.; Zhou, X.; Chen, E.-Q.; Lu, H. Geminal Dimethyl Substitution Enables Controlled Polymerization of Penicillamine-Derived β-Thiolactones and Reversed Depolymerization. *Chem* **2020**, *6*, 1831−1843.

(2) Yuan, P.; Sun, Y.; Xu, X.; Luo, Y.; Hong, M. Towards High-Performance Sustainable Polymers via Isomerization-Driven Irreversible Ring-Opening Polymerization of Five-Membered Thionolactones. *Nat. Chem.* **2022**, *14*, 294−303.

(3) Wang, Y. C.; Zhu, Y. N.; Lv, W. X.; Wang, X. H.; Tao, Y. H. Tough while Recyclable Plastics Enabled by Monothiodilactone Monomers. *J. Am. Chem. Soc.* **2023**, *145*, 1877−1885.

(4) Nakano, K.; Tatsumi, G.; Nozaki, K. Synthesis of Sulfur-Rich Polymers: Copolymerization of Episulfide with Carbon Disulfide by Using [PPN]Cl/(salph)Cr(III)Cl system. *J. Am. Chem. Soc.* **2007**, *129*, 15116−15117.

(5) Su, Y. L.; Yue, L.; Tran, H.; Xu, M. Z.; Engler, A.; Ramprasad, R.; Qi, H. J.; Gutekunst, W. R. Chemically Recyclable Polymer System Based on Nucleophilic Aromatic Ring-Opening Polymerization. *J. Am. Chem. Soc.* **2023**, *145*, 13950−13956.

(6) Hu, Y.; Zhang, L. H.; Wang, Z.; Hu, R. R.; Tang, B. Z. Economical Synthesis of Functional Aromatic Polythioamides from KOH-Assisted Multicomponent Polymerizations of Sulfur, Aromatic Diamines and Dialdehydes. *Polym. Chem.* **2023**, *14*, 2617−2623.

(7) Tian, T.; Hu, R. R.; Tang, B. Z. Room Temperature One-Step Conversion from Elemental Sulfur to Functional Polythioureas through Catalyst-Free Multicomponent Polymerizations. *J. Am. Chem. Soc.* **2018**, *140*, 6156−6163.

(8) Zhang, Q.; Qu, D. H.; Feringa, B. L.; Tian, H. Disulfide-Mediated Reversible Polymerization toward Intrinsically Dynamic Smart Materials. *J. Am. Chem. Soc.* **2022**, *144*, 2022−2033.

(9) Pople, J. M. M.; Nicholls, T. P.; Pham, L. N.; Bloch, W. M.; Lisboa, L. S.; Perkins, M. V.; Gibson, C. T.; Coote, M. L.; Jia, Z.; Chalker, J. M. Electrochemical Synthesis of Poly(trisulfides). *J. Am. Chem. Soc.* **2023**, *145*, 11798−11810.

(10) Chung, W. J.; Griebel, J. J.; Kim, E. T.; Yoon, H.; Simmonds, A. G.; Ji, H. J.; Dirlam, P. T.; Glass, R. S.; Wie, J. J.; Nguyen, N. A.; Guralnick, B. W.; Park, J.; Somogyi, A.; Theato, P.; Mackay, M. E.; Sung, Y. E.; Char, K.; Pyun, J. The Use of Elemental Sulfur as an Alternative Feedstock for Polymeric Materials. *Nat. Chem.* **2013**, *5*, 518−524.

(11) Lee, T.; Dirlam, P. T.; Njardarson, J. T.; Glass, R. S.; Pyun, J. Polymerizations with Elemental Sulfur: From Petroleum Refining to Polymeric Materials. *J. Am. Chem. Soc.* **2022**, *144*, 5−22.

(12) Houk, J.; Whitesides, G. M. Structure Reactivity Relations for Thiol Disulfide Interchange. *J. Am. Chem. Soc.* **1987**, *109*, 6825−6836.

(13) Singh, R.; Whitesides, G. M. Degenerate Intermolecular Thiolate Disulfide Interchange Involving Cyclic Five-Membered Disulfides is Faster by Approximately ~10^3 Than That Involving Six-Membered or Seven-Membered Disulfides. *J. Am. Chem. Soc.* **1990**, *112*, 6304-6309.

(14) Fu, J. Q.; Yu, C. M.; Li, L.; Yao, S. Q. Intracellular Delivery of Functional Proteins and Native Drugs by Cell-Penetrating Poly(disulfide)s. *J. Am. Chem. Soc.* **2015**, *137*, 12153−12160.

(15) Hashim, P. K.; Okuro, K.; Sasaki, S.; Hoashi, Y.; Aida, T. Reductively Cleavable Nanocaplets for siRNA Delivery by Template-Assisted Oxidative Polymerization. *J. Am. Chem. Soc.* **2015**, *137*, 15608−15611.

(16) Qian, L. H.; Fu, J. Q.; Yuan, P. Y.; Du, S. B.; Huang, W.; Li, L.; Yao, S. Q. Intracellular Delivery of Native Proteins Facilitated by Cell-Penetrating Poly(disulfide)s. *Angew. Chem. Int. Ed.* **2018**, *57*, 1532−1536.
(17) Lu, J.; Wang, H.; Tian, Z.; Hou, Y.; Lu, H. Cryopolymerization of 1,2-Dithiolanes for the Facile and Reversible Grafting-from Synthesis of Protein-Polydisulfide Conjugates. *J. Am. Chem. Soc.* **2020**, *142*, 1217−1221.
(18) Trzcinski, J. W.; Morillas-Becerril, L.; Scarpa, S.; Tannorella, M.; Muraca, F.; Rastrelli, F.; Castellani, C.; Fedrigo, M.; Angelini, A.; Tavano, R.; Papini, E.; Mancin, F. Poly(lipoic acid)-Based Nanoparticles as Self-Organized, Biocompatible, and Corona-Free Nanovectors. *Biomacromolecules* **2021**, *22*, 467−480.
(19) Zhang, R. H.; Nie, T. Q.; Fang, Y. F.; Huang, H.; Wu, J. Poly(disulfide)s: From Synthesis to Drug Delivery. *Biomacromolecules* **2022**, *23*, 1−19.
(20) Zhu, Y. W.; Lin, M. Y.; Hu, W. T.; Wang, J. K.; Zhang, Z. G.; Zhang, K.; Yu, B. R.; Xu, F. J. Controllable Disulfide Exchange Polymerization of Polyguanidine for Effective Biomedical Applications by Thiol-Mediated Uptake. *Angew. Chem. Int. Ed.* **2022**, *61*, e2022005.
(21) Lu, J.; Xu, Z.; Fu, H.; Lin, Y.; Wang, H.; Lu, H. Room-Temperature Grafting from Synthesis of Protein-Polydisulfide Conjugates via Aggregation-Induced Polymerization. *J. Am. Chem. Soc.* **2022**, *144*, 15709−15717.
(22) Andren, O. C. J.; Fernandes, A. P.; Malkoch, M. Heterogeneous Rupturing Dendrimers. *J. Am. Chem. Soc.* **2017**, *139*, 17660−17666.
(23) Yu, B. C.; Zheng, Y. Q.; Yuan, Z. N.; Li, S. S.; Zhu, H.; De la Cruz, L. K.; Zhang, J.; Ji, K. L.; Wang, S. M.; Wang, B. H. Toward Direct Protein S-Persulfidation: A Prodrug Approach That Directly Delivers Hydrogen Persulfide. *J. Am. Chem. Soc.* **2018**, *140*, 30−33.
(24) Guo, J.; Zhang, S. Q.; Tao, Y. Q.; Fan, B. E.; Tang, W. Glutathione-Triggered Biodegradable Poly(disulfide)s: Ring-Opening Copolymerization and Potent Antibacterial Activity. *Polym. Chem.* **2022**, *13*, 6637−6649.
(25) Bang, E.-K.; Lista, M.; Sforazzini, G.; Sakai, N.; Matile, S. Poly(disulfide)s. *Chem. Sci.* **2012**, *3*, 1752−1763.
(26) Carnall, J. M. A.; Waudby, C. A.; Belenguer, A. M.; Stuart, M. C. A.; Peyralans, J. J. P.; Otto, S. Mechanosensitive Self-Replication Driven by Self-Organization. *Science* **2010**, *327*, 1502−1506.
(27) Ponnuswamy, N.; Cougnon, F. B. L.; Clough, J. M.; Pantos, G. D.; Sanders, J. K. M. Discovery of an Organic Trefoil Knot. *Science* **2012**, *338*, 783−785.
(28) Zhang, Q.; Shi, C. Y.; Qu, D. H.; Long, Y. T.; Feringa, B.; Tian, H. Exploring a Naturally Tailored Small Molecule for Stretchable, Self-healing, and Adhesive Supramolecular Polymers. *Sci. Adv.* **2018**, *4*, 2375−2548.
(29) Zhang, Q.; Deng, Y. X.; Luo, H. X.; Shi, C. Y.; Geise, G. M.; Feringa, B. L.; Tian, H.; Qu, D. H. Assembling a Natural Small Molecule into a Supramolecular Network with High Structural Order and Dynamic Functions. *J. Am. Chem. Soc.* **2019**, *141*, 12804−12814.
(30) Huang, S.; Shen, Y. K.; Bisoyi, H. K.; Tao, Y.; Liu, Z. C.; Wang, M.; Yang, H.; Li, Q. Covalent Adaptable Liquid Crystal Networks Enabled by Reversible Ring-Opening Cascades of Cyclic Disulfides. *J. Am. Chem. Soc.* **2021**, *143*, 12543−12551.
(31) Barcan, G. A.; Zhang, X.; Waymouth, R. M. Structurally Dynamic Hydrogels Derived from 1,2-Dithiolanes. *J. Am. Chem. Soc.* **2015**, *137*, 5650−5053.
(32) Zhang, X.; Waymouth, R. M. 1,2-Dithiolane-Derived Dynamic, Covalent Materials: Cooperative Self-Assembly and Reversible Cross-Linking. *J. Am. Chem. Soc.* **2017**, *139*, 3822−3833.
(33) Scheutz, G. M.; Rowell, J. L.; Ellison, S. T.; Garrison, J. B.; Angelini, T. E.; Sumerlin, B. S. Harnessing Strained Disulfides for Photocurable Adaptable Hydrogels. *Macromolecules* **2020**, *53*, 4038−4046.
(34) Agergaard, A. H.; Sommerfeldt, A.; Pedersen, S. U.; Birkedal, H.; Daasbjerg, K. Dual-Responsive Material Based on Catechol-Modified Self-Immolative Poly(Disulfide) Backbones. *Angew. Chem. Int. Ed.* **2021**, *60*, 21543−21549.

(35) Choi, C.; Self, J. L.; Okayama, Y.; Levi, A. E.; Gerst, M.; Speros, J. C.; Hawker, C. J.; Read de Alaniz, J.; Bates, C. M. Light-Mediated Synthesis and Reprocessing of Dynamic Bottlebrush Elastomers under Ambient Conditions. *J. Am. Chem. Soc.* **2021**, *143*, 9866−9871.
(36) Albanese, K. R.; Okayama, Y.; Morris, P. T.; Gerst, M.; Gupta, R.; Speros, J. C.; Hawker, C. J.; Choi, C.; de Alaniz, J. R.; Bates, C. M. Building Tunable Degradation into High-Performance Poly(acrylate) Pressure-Sensitive Adhesives. *ACS Macro Lett.* **2023**, *12*, 787−793.
(37) Liu, Y.; Jia, Y.; Wu, Q.; Moore, J. S. Architecture-Controlled Ring-Opening Polymerization for Dynamic Covalent Poly(disulfide)s. *J. Am. Chem. Soc.* **2019**, *141*, 17075−17080.
(38) Zhang, Q.; Deng, Y.; Shi, C.-Y.; Feringa, B. L.; Tian, H.; Qu, D.-H. Dual Closed-Loop Chemical Recycling of Synthetic Polymers by Intrinsically Reconfigurable Poly(disulfides). *Matter* **2021**, *4*, 1352−1364.
(39) Fang, W.; Mu, Z.; He, Y.; Kong, K.; Jiang, K.; Tang, R.; Liu, Z. Organic–Inorganic Covalent–Ionic Molecules for Elastic Ceramic Plastic. *Nature* **2023**, *619*, 293–299.
(40) Clarke, R. W.; Sandmeier, T.; Franklin, K. A.; Reich, D.; Zhang, X.; Vengallur, N.; Patra, T. K.; Tannenbaum, R. J.; Adhikari, S.; Kumar, S. K.; Rovis, T.; Chen, E. Y. X. Dynamic Crosslinking Compatibilizes Immiscible Mixed Plastics. *Nature* **2023**, *616*, 731−739.
(41) Preefer, M. B.; Oschmann, B.; Hawker, C. J.; Seshadri, R.; Wudl, F. High Sulfur Content Material with Stable Cycling in Lithium-Sulfur Batteries. *Angew. Chem. Int. Ed.* **2017**, *56*, 15118−15122.
(42) Rosenthal, E. Q.; Puskas, J. E.; Wesdemiotis, C. Green Polymer Chemistry: Living Dithiol Polymerization via Cyclic Intermediates. *Biomacromolecules* **2012**, *13*, 154−164.
(43) Kandemir, D.; Luleburgaz, S.; Gunay, U. S.; Durmaz, H.; Kumbaraci, V. Ultrafast Poly(disulfide) Synthesis in the Presence of Organocatalysts. *Macromolecules* **2022**, *55*, 7806−7816.
(44) Endo, K.; Yamanaka, T. Copolymerization of Lipoic Acid with 1,2-Dithiane and Characterization of The Copolymer as An Interlocked Cyclic Polymer. *Macromolecules* **2006**, *39*, 4038−4043.
(45) Raeisi, M.; Tsarevsky, N. V. Radical Ring-Opening Polymerization of Lipoates: Kinetic and Thermodynamic Aspects. *J Polym Sci.* **2021**, *59*, 675−684.
(46) Fan, F. Q.; Ji, S. B.; Sun, C. X.; Liu, C.; Yu, Y.; Fu, Y.; Xu, H. P. Wavelength-Controlled Dynamic Metathesis: A Light-Driven Exchange Reaction between Disulfide and Diselenide Bonds. *Angew. Chem. Int. Ed.* **2018**, *57*, 16426−16430.
(47) Pal, S.; Sommerfeldt, A.; Davidsen, M. B.; Hinge, M.; Pedersen, S. U.; Daasbjerg, K. Synthesis and Closed-Loop Recycling of Self-Immolative Poly(dithiothreitol). *Macromolecules* **2020**, *53*, 4685−4691.
(48) Chang, C. C.; Emrick, T. Functional Polyolefins Containing Disulfide and Phosphoester Groups: Synthesis and Orthogonal Degradation. *Macromolecules* **2014**, *47*, 1344−1350.
(49) Kim, S.; Wittek, K. I.; Lee, Y. Synthesis of Poly(disulfide)s with Narrow Molecular Weight Distributions via Lactone Ring-Opening Polymerization. *Chem. Sci.* **2020**, *11*, 4882−4886.
(50) Chao, J. Y.; Yue, T. J.; Ren, B. H.; Gu, G. G.; Lu, X. B.; Ren, W. M. Controlled Disassembly of Elemental Sulfur: An Approach to the Precise Synthesis of Polydisulfides. *Angew. Chem. Int. Ed.* **2022**, *61*, e202115950.
(51) Sakai, N.; Lista, M.; Kel, O.; Sakurai, S.; Emery, D.; Mareda, J.; Vauthey, E.; Matile, S. Self-Organizing Surface-Initiated Polymerization: Facile Access to Complex Functional Systems. *J. Am. Chem. Soc.* **2011**, *133*, 15224−15227.
(52) Wang, B. S.; Zhang, Q.; Wang, Z. Q.; Shi, C. Y.; Gong, X. Q.; Tian, H.; Qu, D. H. Acid-catalyzed Disulfide-mediated Reversible Polymerization for Recyclable Dynamic Covalent Materials. *Angew. Chem. Int. Ed.* **2023**, *62*, e202215329.
(53) Brak, K.; Jacobsen, E. N. Asymmetric Ion-Pairing Catalysis. *Angew. Chem. Int. Ed.* **2013**, *52*, 534−561.
(54) Kniep, F.; Jungbauer, S. H.; Zhang, Q.; Walter, S. M.; Schindler, S.; Schnapperelle, I.; Herdtweck, E.; Huber, S. M. Organocatalysis by Neutral Multidentate Halogen-Bond Donors. *Angew. Chem. Int. Ed.* **2013**, *52*, 7028−7032.
(55) Zhao, Y.; Beuchat, C.; Domoto, Y.; Gajewy, J.; Wilson, A.; Mareda, J.; Sakai, N.; Matile, S. Anion−π Catalysis. *J. Am. Chem. Soc.* **2014**, *136*, 2101−2111.

(56) Marcos, V.; Stephens, A. J.; Jaramillo-Garcia, J.; Nussbaumer, A. L.; Woltering, S. L.; Valero, A.; Lemonnier, J. F.; Vitorica-Yrezabal, I. J.; Leigh, D. A. Allosteric Initiation and Regulation of Catalysis with a Molecular Knot. *Science* **2016**, *352*, 1555−1559.
(57) Eichstaedt, K.; Jaramillo-Garcia, J.; Leigh, D. A.; Marcos, V.; Pisano, S.; Singleton, T. A. Switching between Anion-Binding Catalysis and Aminocatalysis with a Rotaxane Dual-Function Catalyst. *J. Am. Chem. Soc.* **2017**, *139*, 9376−9381.
(58) Banik, S. M.; Levina, A.; Hyde, A. M.; Jacobsen, E. N. Lewis Acid Enhancement by Hydrogen-Bond Donors for Asymmetric Catalysis. *Science* **2017**, *358*, 761−764.
(59) Benz, S.; Poblador-Bahamonde, A. I.; Low-Ders, N.; Matile, S. Catalysis with Pnictogen, Chalcogen, and Halogen Bonds. *Angew. Chem. Int. Ed.* **2018**, *57*, 5408−5412.
(60) Pupo, G.; Ibba, F.; Ascough, D. M. H.; Vicini, A. C.; Ricci, P.; Christensen, K. E.; Pfeifer, L.; Morphy, J. R.; Brown, J. M.; Paton, R. S.; Gouverneur, V. Asymmetric Nucleophilic Fluorination under Hydrogen Bonding Phase-transfer Catalysis. *Science* **2018**, *360*, 638−642.
(61) Sutar, R. L.; Huber, S. M. Catalysis of Organic Reactions through Halogen Bonding. *ACS Catal.* **2019**, *9*, 9622−9639.
(62) Dorel, R.; Feringa, B. Stereodivergent Anion Binding Catalysis with Molecular Motors. *Angew. Chem. Int. Ed.* **2020**, *59*, 785−789.
(63) Ovian, J. M.; Vojackova, P.; Jacobsen, E. N. Enantioselective Transition-Metal Catalysis via an Anion-Binding Approach. *Nature* **2023**, *616*, 84−89.
(64) Zhang, Z. G.; Schreiner, P. R. (Thio)urea Organocatalysis-What Can Be Learnt from Anion Recognition? *Chem. Soc. Rev.* **2009**, *38*, 1187−1198.
(65) De, C. K.; Klauber, E. G.; Seidel, D. Merging Nucleophilic and Hydrogen Bonding Catalysis: An Anion Binding Approach to the Kinetic Resolution of Amines. *J. Am. Chem. Soc.* **2009**, *131*, 17060−17061.
(66) Bergonzini, G.; Schindler, C. S.; Wallentin, C. J.; Jacobsen, E. N.; Stephenson, C. R. J. Photoredox Activation and Anion Binding Catalysis in the Dual Catalytic Enantioselective Synthesis of Bamino Esters. *Chem. Sci.* **2014**, *5*, 112−116.
(67) Samha, M. H.; Wahlman, J. L. H.; Read, J. A.; Werth, J.; Jacobsen, E. N.; Sigman, M. S. Exploring Structure-Function Relationships of Aryl Pyrrolidine-Based Hydrogen-Bond Donors in Asymmetric Catalysis Using Data-Driven Techniques. *ACS Catal.* **2022**, *12*, 14836−14845.
(68) Schafer, A. G.; Wieting, J. M.; Fisher, T. J.; Mattson, A. E. Chiral Silanediols in Anion-Binding Catalysis. *Angew. Chem. Int. Ed.* **2013**, *52*, 11321−11324.
(69) Mancheno, O. G.; Asmus, S.; Zurro, M.; Fischer, T. Highly Enantioselective Nucleophilic Dearomatization of Pyridines by Anion-Binding Catalysis. *Angew. Chem. Int. Ed.* **2015**, *54*, 8823−8827.
(70) Zurro, M.; Asmus, S.; Bamberger, J.; Beckendorf, S.; Mancheno, O. G. Chiral Triazoles in Anion-Binding Catalysis: New Entry to Enantioselective Reissert-Type Reactions. *Chem. Eur. J.* **2016**, *22*, 3785−3793.
(71) Dove, A. P.; Pratt, R. C.; Lohmeijer, B. G. G.; Waymouth, R. M.; Hedrick, J. L. Thiourea-based Bifunctional Organocatalysis: Supramolecular Recognition for Living Polymerization. *J. Am. Chem. Soc.* **2005**, *127*, 13798−13799.
(72) Zhang, X.; Jones, G. O.; Hedrick, J. L.; Waymouth, R. M. Fast and Selective Ring-Opening Polymerizations by Alkoxides and Thioureas. *Nat. Chem.* **2016**, *8*, 1047−1053.
(73) Lin, B.; Waymouth, R. M. Urea Anions: Simple, Fast, and Selective Catalysts for Ring-Opening Polymerizations. *J. Am. Chem. Soc.* **2017**, *139*, 1645−1652.
(74) Lin, B.; Waymouth, R. M. Organic Ring-Opening Polymerization Catalysts: Reactivity Control by Balancing Acidity. *Macromolecules* **2018**, *51*, 2932−2938.
(75) Zhu, J. B.; Chen, E. Y. From meso-Lactide to Isotactic Polylactide: Epimerization by B/N Lewis Pairs and Kinetic Resolution by Organic Catalysts. *J. Am. Chem. Soc.* **2015**, *137*, 12506−12509.

(76) Li, M. S.; Zhang, S.; Zhang, X. Y.; Wang, Y. C.; Chen, J. L.; Tao, Y. H.; Wang, X. H. Unimolecular Anion-Binding Catalysts for Selective Ring-Opening Polymerization of O-carboxyanhydrides. *Angew. Chem. Int. Ed.* **2021**, *60*, 6003−6012.
(77) Lv, W. X.; Wang, Y. C.; Li, M. S.; Wang, X. H.; Tao, Y. H. Precision Synthesis of Polypeptides via Living Anionic Ring-Opening Polymerization of N-Carboxyanhydrides by Tri-thiourea Catalysts. *J. Am. Chem. Soc.* **2022**, *144*, 23622−23632.
(78) Kottisch, V.; Jermaks, J.; Mak, J. Y.; Woltornist, R. A.; Lambert, T. H.; Fors, B. P. Hydrogen Bond Donor Catalyzed Cationic Polymerization of Vinyl Ethers. *Angew. Chem. Int. Ed.* **2021**, *60*, 4535−4539.
(79) Li, M.; Zhang, Z.; Yan, Y.; Lv, W.; Li, Z.; Wang, X.; Tao, Y. Anion-Binding Catalysis Enables Living Cationic Polymerization. *Nat. Synth.* **2022**, *1*, 815−823.
(80) Li, M. S.; Li, H. Y.; Zhang, X. Y.; Wang, X. H.; Tao, Y. H. Mechanistic Insight into Anion-Binding Catalytic Living Cationic Polymerization. *Angew. Chem. Int. Ed.* **2023**, *62*, e202303237.
(81) Fargher, H. A.; Lau, N.; Richardson, H. C.; Cheong, P. H. Y.; Haley, M. M.; Pluth, M. D.; Johnson, D. W. Tuning Supramolecular Selectivity for Hydrosulfide: Linear Free Energy Relationships Reveal Preferential C-H Hydrogen Bond Interactions. *J. Am. Chem. Soc.* **2020**, *142*, 8243−8251.
(82) Macreadie, L. K.; Gilchrist, A. M.; McNaughton, D. A.; Ryder, W. G.; Fares, M.; Gale, P. A. Progress in Anion Receptor Chemistry. *Chem* **2022**, *8*, 46−118.
(83) Singh, R.; Whitesides, G. M. Comparisons of Rate Constants for Thiolate-Disulfide Interchange in Water and in Polar Aprotic-Solvents Using Dynamic ^{1}H NMR Line-Shape Analysis. *J. Am. Chem. Soc.* **1990**, *112*, 1190−1197.
(84) Singh, R.; Whitesides, G. M., Thiol-disulfide interchange. In *Supplement S: The Chemistry of Sulfur-Containing Functional Groups*; Patai, S., Rapport, Z., Eds.; Wiley, 1993.
(85) Liu, Y.; Sengupta, A.; Raghavachari, K.; Flood, A. H. Anion Binding in Solution: Beyond the Electrostatic Regime. *Chem* **2017**, *3*, 411−427.
(86) Wang, Y. H.; Cao, Z. Y.; Li, Q. H.; Lin, G. Q.; Zhou, J.; Tian, P. Activating Pronucleophiles with High pKa Values: Chiral Organo-Superbases. *Angew. Chem. Int. Ed.* **2020**, *59*, 8004−8014.
(87) Small high-molecular-weight shoulders were observed in GPC traces and were attribute to residual chain transfer. See Supporting Information S.10 for detail analysis.
(88) Lidston, C. A. L.; Abel, B. A.; Coates, G. W. Bifunctional Catalysis Prevents Inhibition in Reversible-Deactivation Ring-Opening Copolymerizations of Epoxides and Cyclic Anhydrides. *J. Am. Chem. Soc.* **2020**, *142*, 20161−20169.
(89) Darensbourg, D. J. Chain transfer agents utilized in epoxide and CO_2 copolymerization processes. *Green Chem.* **2019**, *21*, 2214−2223.
(90) Waser, J.; Gaspar, B.; Nambu, H.; Carreira, E. M. Hydrazines and Azides via the Metal-Catalyzed Hydrohydrazination and Hydroazidation of Olefins. *J. Am. Chem. Soc.* **2006**, *128*, 11693−11712.
(91) Wang, X. Q.; Tong, R. Facile Tandem Copolymerization of *O*-Carboxyanhydrides and Epoxides to Synthesize Functionalized Poly(ester-*b*-carbonates). *J. Am. Chem. Soc.* **2022**, *144*, 20687−20698.
(92) Alassad, Z.; Nandi, A.; Kozuch, S.; Milo, A. Reactivity and Enantioselectivity in NHC Organocatalysis Provide Evidence for the Complex Role of Modifications at the Secondary Sphere. *J. Am. Chem. Soc.* **2022**, *145*, 89−98.
(93) Wang, M.; Simon, J. C.; Xu, M.; Corio, S. A.; Hirschi, J. S.; Dong, V. M. Copper-Catalyzed Hydroamination: Enantioselective Addition of Pyrazoles to Cyclopropenes. *J. Am. Chem. Soc.* **2023**, *145*, 14573−14580.
(94) Zell, M. T.; Padden, B. E.; Paterick, A. J.; Thakur, K. A. M.; Kean, R. T.; Hillmyer, M. A.; Munson, E. J. Unambiguous Determination of the ^{13}C and ^{1}H NMR Stereosequence Assignments of Polylactide Using High-Resolution Solution NMR Spectroscopy. *Macromolecules* **2002**, *35*, 7700−7707.
(95) Orhan, B.; Tschan, M. J.; Wirotius, A. L.; Dove, A. P.; Coulembier, O.; Taton, D. Isoselective Ring-Opening Polymerization of rac-Lactide from Chiral Takemoto's Organocatalysts: Elucidation of Stereocontrol. *ACS Macro Lett.* **2018**, *7*, 1413−1419.

(96) The overlapping ^{1}H signals precludes the use of decoupled ^{1}H NMR analysis. And ^{1}H-^{13}C HMBC cannot reveal correlation across S−S bond to distinguish different triads.
(97) Rabenstein, D. L.; Theriault, Y. A Nuclear Magnetic-Resonance Study of the Kinetics and Equilibria for the Oxidation of Penicillamine and N-Acetylpenicillamine by Glutathione Disulfide. *Can. J. Chem.* **1984**, *62*, 1672−1680.